Modeling the Activity of Wax Inhibitors: A Case Study of Poly(octadecyl acrylate)

D. M. Duffy* and P. M. Rodger

Department of Chemistry, University of Warwick, Coventry, CV4 7AL U.K.

Received: July 11, 2002

The role of poly(octadecyl acrylate) in inhibiting wax formation and growth has been examined using both molecular dynamics and Monte Carlo methods. The simulations show that the defective wax growth identified in earlier studies[4,6] has a simple energetic basis and indicates that the comblike polymeric inhibitors favor the formation island defects on the wax surface. These island defects have weak interactions with the surrounding crystal, and so act as impurity sites for blocking growth steps. Using the information gained from molecular dynamics simulations of wax growth at a wax/liquid heptane interface, we have generalized recent Monte Carlo growth methods to provide a realistic yet simple model of wax inhibition. The model predicts that poly(octadecyl acrylate) will prevent growth at low supersaturations, where growth occurs largely at step defects, and slows growth at higher supersaturations, where island nucleation is important.

1. Introduction

The presence of impurities can often alter the growth rate and properties of crystals formed from solution. Indeed, there are many chemical processes that seek to exploit added "impurities" to manufacture crystals with desired properties. Clearly an understanding of the mechanism by which such additives work is essential if one hopes to control the resulting crystal properties effectively. Additives that slow crystal growth, or even prevent crystal nucleation, are known as inhibitors and can be found in areas as diverse as biological applications (e.g., kidney stone inhibitors) and scale prevention (lime scale in water pipes).

The central focus of this paper is on controlling the deposition of wax from oil. Wax formation can cause a number of problems, for example, in the transport of crude oil or the operation of diesel engines at low temperatures. Experiments have demonstrated that some comb polymers will inhibit the formation of paraffin crystallites from hydrocarbon solutions. In particular, such polymers have been shown to increase the solubility of long chain alkanes in heptane solution[1] and to increase the meta-stable zone width of wax molecules in solution.[2] Strong evidence is also found in the work of Kern and Dassonville, who showed that adding oligomers of a polyalkylacrylate, $M_w \approx 2000-3000$ u, to C_{36} paraffin/heptane solutions inhibited wax growth and ultimately resulted in smaller paraffin crystals with corrugated faces.[3] However, the molecular structural changes induced by the comb polymers can only be inferred from these studies, and so detailed molecular-level mechanistic information is still needed if the full potential of comb polymers for preventing wax deposition is to be realized.

To understand the inhibitor mechanism, we have previously used molecular simulation methods to study the interaction of poly(octadecyl acrylate) (PA-18) oligomers with the surfaces of an octacosane (n-$C_{28}H_{58}$, also denoted n-C_{28} in this paper) crystal. In the initial studies,[4] dimers of PA-18 were found to adsorb strongly onto the (100), (010), and (110) faces of n-C_{28} alkane crystals. When more alkane molecules were subsequently added to the surface to simulate wax growth, the PA-18 dimers were found to induce substantial localized distortion in the structure of the wax growth, particularly disrupting the lamellar structure of the crystal; this lamellar structure has been identified as characteristic of alkane waxes.[5] More detailed calculations were then performed with PA-18 octamers, at both wax/vacuum and wax/liquid heptane interfaces.[6] The octamer was found to discriminate between the different wax surfaces much more strongly than the dimer, with adsorption most favored on the two main growth surfaces: (010) and (110). Subsequent addition of n-C_{28} to the inhibited surfaces showed an even stronger disruption of the wax structure than was observed with the PA-18 dimer. In particular, shear defects developed quickly when complete wax layers were added to the inhibited surface, with alkane molecules above the inhibitor shifting to align with the inhibitor rather than with the underlying wax crystal structure. The evolution of these shear defects was most facile at the wax/liquid heptane interface. In comparison, simulated growth on the uninhibited surface was entirely commensurate with the underlying crystal structure, both with and without solvent present at the interface. It was concluded that the induction of this lateral shift in the alkane layers and consequent disruption of the lamellar structure was fundamental to the activity of the inhibitors.

In this paper, we show that the shear defects identified in the earlier studies can be understood on energetic grounds: it is energetically more favorable for alkane molecules to adsorb over the inhibitor rather than across its edges, so that the adsorption of the polymeric inhibitor will nucleate island defects on the growth surface. The pinning of growth steps by such defects is a well-established mechanism for growth inhibition and was first discussed by Cabrera and Vermilyea.[7] They demonstrated that the width of the dead zone is inversely proportional to the impurity separation. More recent Monte Carlo (MC) investigations[8,9] have established the presence of a dead zone for both rough growth and step growth. Step blocking by dilute concentrations of impurities has been studied experimentally for a number of systems.[8,10,11]

The purpose of this paper is to identify an inhibitor mechanism and then to encapsulate the mechanism into a simple MC growth model. In sections 3 and 4, we establish that the inhibitor

* To whom correspondence should be addressed. Current address: Department of Physics and Astronomy, University College London, Gower Street, London, WC1E 6BT, U.K.

10.1021/jp026501j CCC: $22.00
Published on Web 10/03/2002

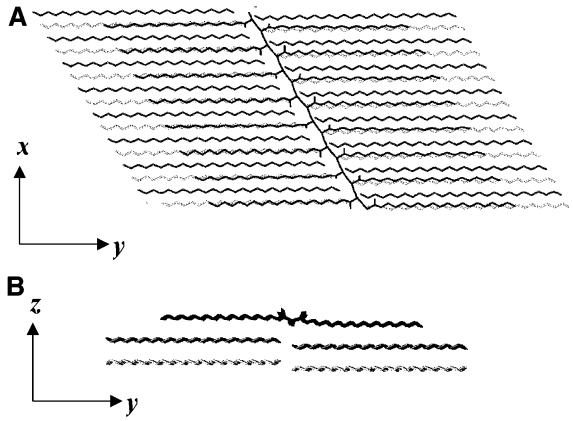

Figure 1. Top (a) and side (b) views of a poly(octadecyl acrylate) inhibitor adsorbed on a (010) surface of an octacosane crystal. The polymer is shown in black, the top crystal layer is shown in dark gray, and the lower crystal layer is shown in light gray.

mechanism involves PA-18 oligomers acting as nucleation sites for island defects that subsequently pin the growth steps. We then show, in section 5, how the MC method of van Enckevort and co-workers[9] can be generalized to study growth inhibition in paraffin crystals. The parameters required for the model are obtained directly from atomistic MD simulations of surfaces and surface steps. The simulations presented herein demonstrate unambiguously that adsorbed immobile inhibitor molecules do block step growth in paraffin crystals and can completely prevent growth for reasonable values of the supersaturation.

2. Calculation Details

MD calculations were performed using the DL_POLY simulation package,[12] which employs standard MD procedures[13] to model the properties of materials. We used an *NVT* ensemble with a Nose-Hoover thermostat (relaxation time $\tau = 0.01$ ps) to maintain an average temperature of 293 K. A 2 fs time step was used for all simulations. The potentials and protocols were the same as those described in previous publications[4,6,14] but are reproduced here for completeness.

The octacosane crystal substrate was modeled using an array of $8 \times 9 \times 2$ *n*-C_{28} molecules (molecular formula $C_{28}H_{56}$) with a monoclinic crystal structure; the lattice parameters $a = 5.05$ Å, $b = 7.57$ Å, $c = 37.89$ Å, and $\gamma = 121°$ were obtained from *NPT* molecular dynamics calculations with the potential described below and interpolate reasonably between the published structures for *n*-C_{20} and *n*-C_{36}.[15] Periodic boundary conditions were imposed in the $a-c$ plane, giving a 2-dimensional crystal slab with two (010) surfaces. This slab may be described as having nine layers, each consisting of two lamellae of eight molecules (see Figure 1).

An inhibited surface was modeled by adsorbing a hexadecamer of PA-18 (i.e., poly(octadecyl acrylate), **1**) onto the top (010) surface; the hexadecamer gives complete coverage of the model surface and the backbone bonds across the periodic boundary to produce an infinite polymer. Earlier calculations demonstrated excellent matching between finite oligomers (dimer and octamer) of PA-18 and the (010) octacosane surface; the current calculations demonstrate that the match remains excellent for larger polymer units. The structure of the adsorbed polymer is shown in Figure 1. In the following text, we will adopt a convention in which *z* denotes the surface normal, *y* is parallel to the long axis of the *n*-C_{28} molecules, and *x* is in the plane of the surface and perpendicular to the *n*-C_{28} long axis.

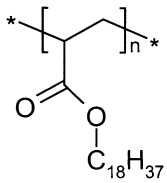

1: poly (octadecyl acrylate)

Full details of the intermolecular potentials are given elsewhere.[4] The potentials used united atoms to describe the *n*-C_{28} and PA-18 alkyl side chains. Parameters were taken from Moller et al.[16] but with the bond angle adjusted to 112.5° by fitting to the location of the first three peaks in the C−C radial distribution functions for crystalline *n*-$C_{20}H_{42}$ and *n*-$C_{36}H_{74}$.[17] Although it is generally considered that all atom potentials are required for quantitative modeling of alkane solids, the semiquantitative united atom potentials described above are appropriate for this study because of the generic nature of the problem: waxes will form from many different alkane mixtures and can be inhibited by a range of different poly(alkyl acrylates). Thus, to identify the common influences responsible for wax inhibition, the main requirements are that the alkyl chain interactions be treated consistently and with a potential that gives at least a semiquantitative description of paraffin liquid and crystal structures. A united atom potential does satisfy these requirements and reduces computational time by an order of magnitude. The PA-18 backbone (including acrylate groups) was modeled with all atom CHARMm parameters; charges were calculated from a Gaussian 92 6_31G** calculation of a monomer in which the C_{18} side chain was replaced by a methyl group.

All bonds were constrained using the SHAKE algorithm,[13] whereas bond angles and torsions were treated flexibly. van der Waals interactions were represented using a Lennard Jones potential with a cutoff of 12 Å, and electrostatics were calculated using a direct Coulomb sum with a cutoff of 17 Å. The direct Coulomb summation was chosen as the only option within DL_POLY that was compatible with 2-D, rather than 3-D, periodicity. It was feasible to use the direct Coulomb summation in this system because the electrostatics are such a limited part of the system: electrostatic interactions will only influence PA-18 properties, and for the adsorbed polymer, these were found to be dominated by the influence of the wax surface; also, the trial calculations with an EWALD sum showed little difference in the polymer properties.

To examine inhibition at a wax/liquid hydrocarbon interface, a heptane film was condensed onto the wax surface using an external potential of the form:

$$V(z) = {}^1/_2\, k\,(z - z_0)^2 \qquad z > z_0$$

$$V(z) = 0 \qquad z < z_0$$

where $k = 0.1$ kJ mol^{-1} Å^{-1} and z was measured from the top layer of the crystal. z_0 was taken as 31 Å. The potential served only to create the liquid film, and it did not affect the properties beyond the low-density region near the liquid surface; indeed, subsequent calculations of the liquid heptane film with and without this confining potential showed no structural or dynamic differences.[14] The intermolecular and intramolecular potentials used for the solvent were the same as those used for the *n*-C_{28}.

3. Energetic Considerations for Inhibited Wax Growth

The origin of the shear defects in inhibited wax growth noted above was examined by considering the energetics of adding

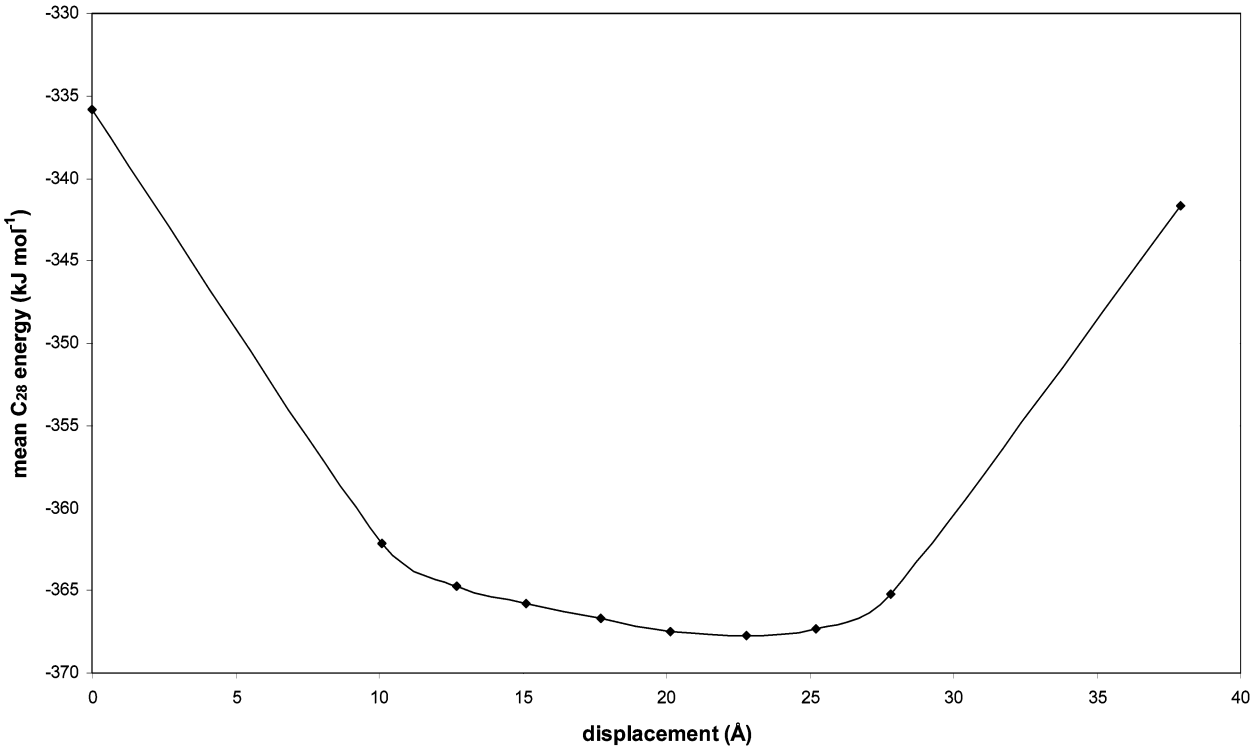

Figure 2. Mean molecule energy of a lamella of *n*-C_{28} molecules over a PA-18 polymer adsorbed on a (010) octacosane surface, plotted against displacement along the long axis of the crystal molecules (*y* direction). The origin of the displacement is defined as the position commensurate with the underlying crystal.

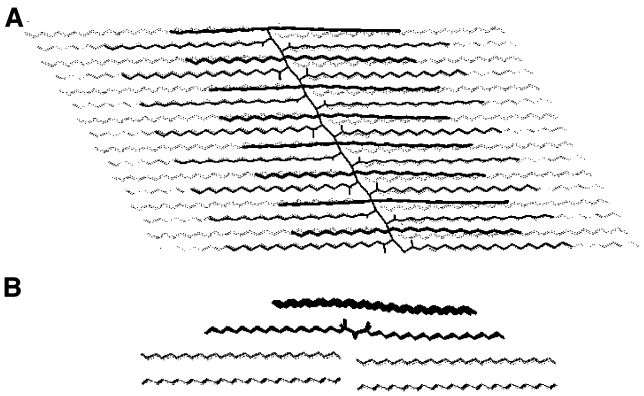

Figure 3. Top (a) and side (b) views of the minimum energy configuration of an alkane layer over an adsorbed PA-18 inhibitor. The alkane layer is shown in thick black lines, the polymer is shown in thin black lines, and the upper crystal layers are shown in gray lines.

n-C_{28} molecules to an inhibited surface. A single lamella, containing one layer (eight molecules) of *n*-C_{28}, was placed 6 Å above the inhibited surface at a series of lateral displacements in the range $0 < y < 40$ Å; values of $y = 0$ and 37.9 Å define the positions that would be expected in growing a perfect crystal (see Figure 1). The lamella was then relaxed onto the surface using very low-temperature MD simulations ($T = 2$ K)[18] for 8 ps, and the average molecule energy for the final 6 ps was calculated. The resulting energy is plotted against the lateral (*y*) displacement in Figure 2. The high energy at $y = 0$ and 38 Å corresponds to adding a wax lamella in a position commensurate with the underlying crystal structure. The energy falls rapidly as the lamella is moved onto the inhibitor and there is a broad minimum for positions in which the lamella lies wholly over the inhibitor. The structure corresponding to the minimum energy position ($y \approx 23$ Å) is illustrated in Figure 3. These results are entirely consistent with the MD simulations of inhibited growth reported earlier,[6] and indeed the magnitude of the energy barrier seen in Figure 2 explains the rapidity with which the shear defect formed in those simulations.

It is important to note that the preceding discussion relates only to wax growth in the vicinity of an adsorbed inhibitor and need not imply that alkanes will add over the inhibitor in preference to a clean wax surface. However, once the inhibitor is adsorbed onto a wax surface, subsequent growth would need either to displace or cover the inhibitor. For oligomeric and larger inhibitors, there are likely to be multiple adsorbed side chains, and so displacement is unlikely. Thus, it will be the energetics of growing over the inhibitor (as per Figure 2) that will limit crystal growth. Given the high energy penalty of adding paraffin over the end of the inhibitor and commensurate with the underlying wax (Figure 2), we postulate that the inhibitor acts as a source of island defects. A schematic representation of the proposed inhibitor mechanism is shown in Figure 4.

4. Properties of Island Defects

In the previous section, we demonstrated that it is energetically favorable for alkanes to attach to an inhibited surface in a position that is incommensurate with the underlying crystal. Such molecules would therefore tend to nucleate island defects on the wax surface. As will be shown in the next section, it is possible to formulate simple yet effective Monte Carlo inhibited growth models from a knowledge of the energy of these island defects. As a prerequisite, we first report the properties of such island defects calculated directly from MD simulations. Results are reported for islands with one to three alkane layers, both on the adsorbed PA-18 polymer and on a clean surface. For the clean surface, the island was commensurate with the underlying crystal, whereas for the inhibited surface, it was located over the inhibitor. The properties of the molecules near a nondefective

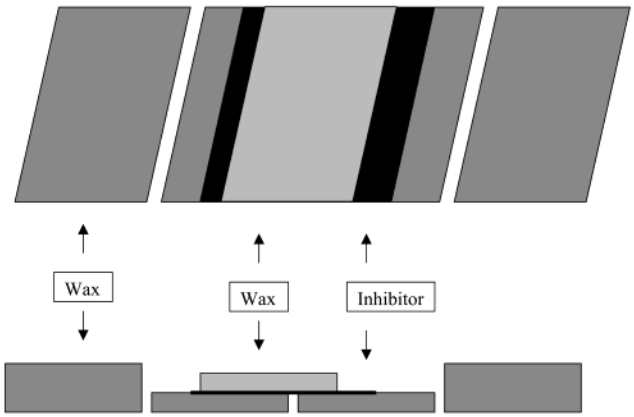

Figure 4. Schematic representation of a model of inhibited crystal growth. The crystal lamellae are shown in dark gray, the inhibitor is shown in black, and the incommensurate growth over the inhibitor is shown in light gray.

planar surface were also calculated for comparison. All calculations were repeated in the presence of liquid heptane in order to study solvent effects. In the following discussion, we adopt a notation in which layer 1 always refers to the uppermost layer (i.e., the layer exposed to the vacuum or liquid heptane).

The islands on the inhibitor were created by adding the specified number of layers of octacosane at a height of 6 Å above the inhibited surface and with a lateral displacement corresponding to the lowest energy position found in section 3 ($y \approx 23$ Å). The layers were relaxed onto the surface using a low temperature (10 K), 20 ps MD simulation. A 200 ps simulation at a temperature of 293 K was then performed, and the energy and coordinates of the molecules were recorded every 0.5 ps during the final 150 ps for subsequent analysis. The molecules of the island, the inhibitor, and the top layer of crystal were mobile during the simulation while the lower crystal layers were frozen. Convergence tests indicated that freezing the substrate has a significant effect only on the energies of the two layers adjacent to the frozen layers, and so the properties of the islands were not affected by this frozen boundary.

Islands were also created on a clean surface. In this case, the lamellae were added in a position commensurate with the crystal substrate to form islands one to three layers high on the (010) surface. The island molecules and the top two crystal layers were mobile during a 200 ps, 293 K simulation and the lower five crystal layers frozen. The energies and coordinates of each molecule in the islands were again captured every 0.5 ps for subsequent analysis. Snapshots of the simulations of the three layer islands with solvent on the inhibitor and on the clean surface are shown in Figure 5.

The Hartmann Perdok theory of crystal growth[19] states that the rate of growth of a crystal face is proportional to the energy gained by adding a layer of molecules to that face, because molecules will attach preferentially to low energy sites on high energy surfaces. The relative energies of the molecules in an island on a clean surface and an inhibited surface should, therefore, give an indication of the relative rates of nucleation on the two island types.

Average potential energies for molecules within layer i of an island, E_i, were calculated by first determining the time-averaged energy of each molecule j within layer i during the final 150 ps of the simulation, $E_i(j)$, and then averaging these $E_i(j)$ over all molecules j within the specified layer i. Uncertainties were estimated from the standard deviation of $E_i(j)$ across all molecules j within the specified layer i. The results are

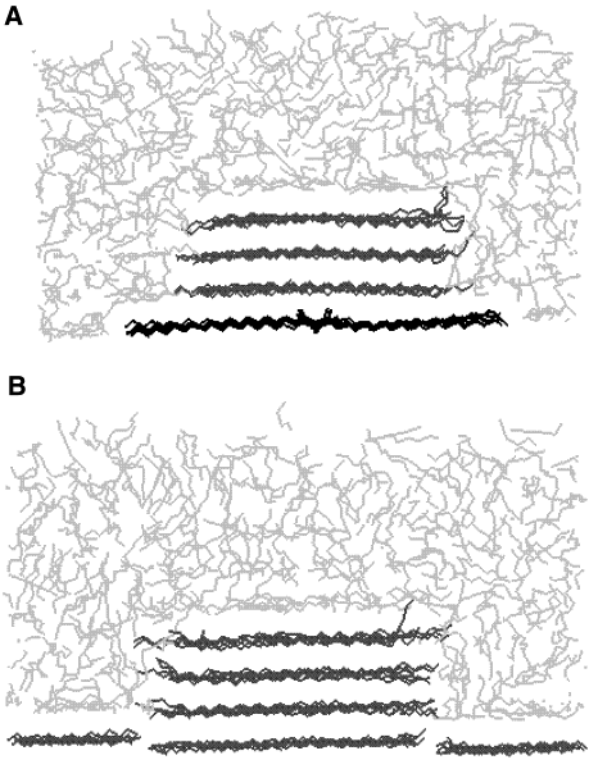

Figure 5. Side-view snapshots of the MD simulations of three-layer islands on a (010) octacosane surface with (a) and without (b) an adsorbed PA-18 inhibitor in a heptane environment. The *n*-C_{28} molecules are shown in gray, the heptane film is shown light gray, and the inhibitor (a only) is shown in black.

summarized in Table 1 for the clean surface and in Table 2 for the inhibited surface.

Similar trends in E_i were observed for islands on the clean and on the inhibited surfaces, and in many cases, these trends are as expected. The energy of the surface layer on the island (layer 1) was found to increase (i.e., become less favorable) with the height of the island. This is simply because the neighboring *n*-C_{28} molecules in the adjacent lamella are missing. Likewise, the molecule energy decreases with depth into the island, again because of changes in the number of nearest- and next-nearest-neighbors. These trends are very clear for the islands in a vacuum. They are still apparent, albeit with reduced magnitude, in the presence of solvent, where the absence of neighboring *n*-C_{28} molecules is partially compensated by the presence of liquid heptane.

Much more interesting results are apparent from a comparison between the molecule energies of islands on clean and inhibited surfaces. For almost all of the island/layer combinations, E_i is lower (i.e. more favorable) on the inhibited surface than it is on the clean surface. The one exception to this is the surface layer (layer 1) of a solvated three-layer island, where any difference is not statistically significant. It is particularly interesting to note the difference for the single layer islands (height = 1), because these would form a nucleus for step-growth on a clean surface. The results in Tables 1 and 2 indicate that adding a paraffin lamella on top of the inhibitor is actually 11.1 (vacuum) or 11.7 kJ mol^{-1} (solvent) more favorable than laying down a lamella on the clean surface. Thus, at low supersaturations and in the presence of an inhibitor, alkanes would deposit preferentially onto the adsorbed inhibitor where they cannot generate step growth. Because step growth is usually the dominant growth mechanism at low supersaturations, the

TABLE 1: Mean Molecule Energy for Island Defects on a Clean (010) Octacosane Surface under a Vacuum and in the Presence of a Liquid Heptane Film[a]

	mean molecule energy (kJ mol^{-1}) for an island on a clean surface					
	vacuum			solvent		
island height	layer 1	layer 2	layer 3	layer 1	layer 2	layer 3
1	−263.8 (3.3)			−379.6 (3.4)		
2	−259.5 (4.6)	−409.5 (2.3)		−381.3 (4.3)	−434.0 (3.1)	
3	−254.8 (5.4)	−399.8 (3.6)	−424.7 (3.3)	−379.8 (5.6)	−431.1 (2.8)	−441.8 (3.0)
flat surface	−280.4 (4.1)	−428.6 (2.4)	−447.1 (2.0)	−384.0 (4.9)	−440.6 (2.0)	−450.5 (1.8)

[a] Layer 1 signifies the top layer of the island (i.e., at the vacuum or solvent interface), and layers 2 and 3 signify the second and third layers, respectively. The flat surface refers to the equivalent energies for the molecules within a perfect, clean, surface. The numbers in brackets are the standard deviations of the mean molecule energy within the layer (see text).

TABLE 2: Mean Molecule Energy for Island Defects on an Inhibited (010) Octacosane Surface, under a Vacuum and in the Presence of a Liquid Heptane Film[a]

	mean molecule energy (kJ mol^{-1}) for an island on an inhibited surface					
	vacuum			solvent		
island height	layer 1	layer 2	layer 3	layer 1	layer 2	layer 3
1	−274.9 (4.0)			−391.3 (2.9)		
2	−262.7 (3.0)	−420.6 (1.8)		−382.9 (3.2)	−440.5 (5.4)	
3	−260.8 (2.3)	−404.6 (3.2)	−436.4 (1.6)	−377.8 (6.1)	−434.0 (3.1)	−449.7 (2.4)

[a] Layer 1 signifies the top layer of the island, and layers 2 and 3 signify the second and third layers, respectively. The numbers in brackets are the standard deviations of the mean molecule energy within the layer.

presence of the inhibitor will lead to a reduction in the rate of crystal growth.

The comparison of molecule energies for islands and complete surfaces is also instructive. Although island formation is energetically favored over the inhibitor, it is still the case that the formation of complete paraffin layers is energetically the most favorable. This is consistent with the prevalence of step defect driven growth for the paraffin crystals. Again there is one exception, and this may be highly significant for the inhibitor mechanism. It is actually about 8 kJ mol^{-1} more favorable to place a single lamella of paraffin on top of the inhibitor than to have this lamella in the clean surface; the difference is even bigger (about 20 kJ mol^{-1}) in a vacuum. Thus, it is highly likely that any PA-18 adsorbed onto a wax surface will be covered by a paraffin lamella, with subsequent disruption to the growth of the paraffin crystal.

5. Monte Carlo Simulations

From the results of the preceding sections, it has been possible to propose a molecular mechanism for wax inhibition, in which adsorbed polymeric inhibitors create immobile impurities on the crystal surfaces and thereby hinder processes such as step growth. To assess the full impact of such a mechanism, it is useful to have a more course-grained model for the crystal growth that is faster to calculate and therefore allows the growth process to be modeled over longer time scales than are accessible to direct MD simulation. In this section, we show how the Monte Carlo (MC) models that have been used successfully to study crystal growth,[20] with impurities,[8] in more isotropic systems can be extended to model wax inhibition.

The essence of these MC growth methods is that crystal growth or dissolution is modeled by a series of random attempts to add or remove a molecule from the surface. The probability of successfully removing a molecule from the surface is related to the adsorption energy for that molecule, and in the simplest models, this is determined by the number of nearest-neighbors that molecule has within the plane of the surface: a single molecule adsorbed onto a surface is much easier to remove than one that is part of an adsorbed dimer or trimer. The probability of successful addition is governed by the chemical potential driving force and acts as an experimental control variable in much the same way as the degree of supersaturation is used experimentally. For growth of a cubic crystal, this leads to addition and removal probabilities of the form

$$P_i^+ = \nu \exp\{\Delta\mu/kT\}$$

$$P_i^- = \nu \exp\{(2 - j)2\phi/kT\}$$

where ϕ is the in-plane interaction energy between a molecule and its neighbor (termed a "bond" energy by Gilmer and Bennema[19]), j is the number of such neighbors, and ν is a material-dependent constant. For a simple cubic system, the maximum number of in-plane neighbors is four, and so the factor $(2 - j)$ ensures that isolated adsorbed molecules are easily removed. The method has recently been extended to include impurities by van Enckevort and van der Berg[9] (vEvdB) by treating the impurities as sites that do not interact favorably with the growing crystal. In the simplest case, they set $\phi = 0$ for an impurity neighbor.

The method of vEvdB can be generalized to inhibited wax growth. For the (010) and (110) surfaces of paraffin crystals, each added molecule will have up to four nearest neighbors, but the two end-to-end interactions will be much weaker than the two side-by-side interactions. Thus, the probability of a successful removal should be modified to

$$P_i^- = \nu \exp\{[(1 - j_x)2\phi_x + (1 - j_y)2\phi_y]/kT\}$$

where ϕ_x is the side-by-side nearest-neighbor interaction energy and ϕ_y is the corresponding end-to-end energy, j_x is the number of side neighbors, and j_y is end neighbors for the ith n-C_{28} molecule. The method of vEvdB for including impurities, setting $\phi = 0$ where the neighbor is an impurity, is again appropriate for wax inhibition with PA-18. As seen in Figure 1, PA-18 does not completely cover the lamellae to which it is adsorbed, and so end-to-end interactions between the PA-18 and a n-C_{28} molecule on a neighboring lamella will be negligible. Side-by-side interactions with the inhibitor will also be reduced because

of the shorter size of the polymer side chain. In fact, PA-18 polymers are unlikely to adsorb completely onto the surface; instead, there will be tails and loops of PA-18 leading away from adsorbed patches, and these will make it extremely unlikely that *n*-C_{28} molecules will add to the surface beside the adsorbed polymer. Thus, to a good approximation, we expect $\phi_x = \phi_y = 0$ where the neighbor is the inhibitor.

To implement this method we have calculated values for $\phi_{x,y}$ from MD simulations of steps on a solvent covered wax surface. For example, the energy difference between a molecule within the surface plane of a perfect surface and that within an island of height 1 as described in section 4 is that the latter has lost two end-to-end nearest-neighbor interactions. Thus, from the height = 1 and flat surface results in Table 1, we would estimate $2\phi_y = 4.4$ kJ mol^{-1}. In fact, the data in Table 1 shows large statistical uncertainties, and so much longer simulations (5 ns instead of 150 ps) were used to calculate $\phi_x = 5.0$ kJ mol^{-1} and $\phi_y = 1.75$ kJ mol^{-1}.

The following protocol was adopted to implement the MC growth simulations. The crystal surface was treated as a set of 50×50 lattice points, which were assumed to lie in the $x-y$ plane. To be consistent with the preceding discussion of P_i^-, the long axis of the *n*-C_{28} molecules in the crystal was assumed to lie along the *y* axis.

A simulation consisted of 10^9 MC cycles, where each cycle consisted of (1) choosing between attempting an addition or removal (equal probability); (2) picking a surface site (addition) or surface molecule (removal) at random; (3) calculating the appropriate addition or removal probability; and (4) generating a random number that is uniform on the interval [0,1]; if this is smaller than the probability calculated in step 3, then accept the addition/removal event.

To calculate the removal probability, it is necessary to know the height of the surface at the four neighboring lattice sites. For sites within the 50×50 array, this will already be known from the history of the calculation, but for sites on the edge of the array, it is necessary to introduce some sort of boundary conditions. The simplest boundary condition would be to assume 2-D periodicity, in which case the height at each grid point, $H(x,y)$ would be related according to

$$H(x,y) = H(x + 50,y) = H(x,y + 50)$$

where the "50" is the size of the calculation lattice. To facilitate step growth, we have modified these conditions slightly so that

$$H(x,0) = H(x,50) + 1$$

This ensures that there is always at least one step defect on the surface, and so obviates the need to nucleate the surface steps.

A number of different simulations were performed to determine the effect of both $\Delta\mu$ and inhibitor size on the consequent crystal growth. For this purpose, each poly(alkyl acrylate) molecule, **1**, was treated as a set of $n \times 2$ ($x \times y$) lattice sites on which alkanes would not adsorb and that did not interact with neighboring sites. In reality, some growth will occur on the inhibitor, but the incommensurate nature of such growth would ensure there is little interaction with the surrounding crystal, and so growth on the inhibitor may be neglected. On a larger scale, the mixture of on- and off-inhibitor growth sites is likely to determine the porosity of the resulting wax, but this will be on much larger length scales than have been simulated in these calculations. Four equally spaced oligomers were used to inhibit a surface. Simulations were performed for $n = 10$, 15, and 20 and for $\Delta\mu/kT$ in the range 0−0.3; simulations were also performed on an uninhibited surface for comparison.

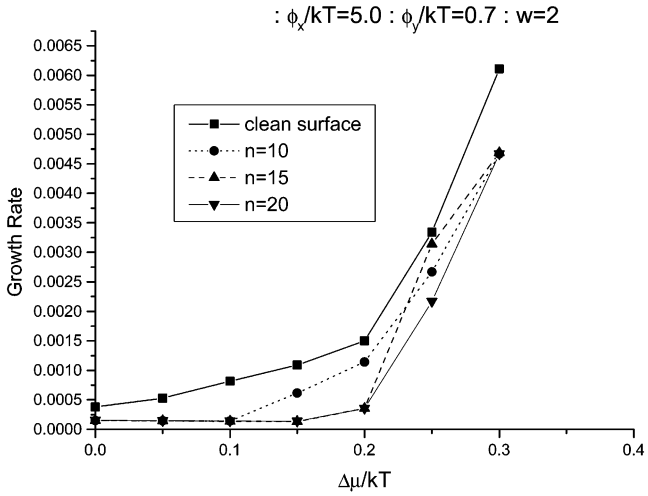

Figure 6. Growth rate versus excess chemical potential for MC simulations of growth with immobile impurities 2 growth units wide ($w = 2$) and 10, 15, and 20 growth units long. The bond strengths parallel (ϕ_y) and perpendicular (ϕ_x) to the molecule long axis are 0.7 and 5.0 kT, respectively. The clean surface is included for comparison.

The average growth rate for the crystal can be calculated from these MC simulations by comparing the number of successful addition (N^+) and removal (N^-) events. Following Gilmer and Bennema,[19] we have defined the growth rate, *R*, as

$$R = (N^+ - N^-)/N^+$$

This definition is very convenient for the growth regime, where it gives values in the range $0 = R = 1$, although it should be noted that it is not so appropriate for dissolution.

The average growth rate has been calculated from the final 2×10^8 cycles of each simulation, and the results are plotted against the $\Delta\mu$ in Figure 6. The growth of the clean surface clearly shows two regimes. For low supersaturations ($\Delta\mu/kT < 0.2$), *R* is small and varies linearly with $\Delta\mu/kT$, whereas at high supersaturation, the growth is much more rapid and varies nonlinearly with the chemical potential driving force. The changeover between these two regimes occurs at $\Delta\mu/kT = 0.2$ and corresponds to the onset of island nucleation to supplement the step growth seen at low supersaturations. The final configuration for $\Delta\mu/kT$ is shown in Figure 7a. The growth step is well defined, but a number of small islands are also apparent, the largest of which spans the periodic boundary across the $x = 0$ edge.

The effect of inhibitor size is also shown in Figure 6. For $n = 15$ and 20, no crystal growth is observed in the entire step growth regime ($\Delta\mu/kT < 0.2$), whereas it is seen only at higher supersaturations ($\Delta\mu/kT < 0.1$) for smaller polymeric inhibitors ($n = 10$). The final configurations for $\Delta\mu/kT = 0.2$ for these three inhibitor sizes are shown in Figure 7b−d. For the smallest polymer (Figure 7b), the inhibitor has clearly slowed growth but the step has successfully grown past this "impurity" barrier. The average height for this surface is 2.6 layers, compared with 3.6 layers for the uninhibited surface. For the larger polymers (Figure 7c,d), it is clear that the steps do not grow beyond the adsorbed inhibitors; however, island nucleation between the steps is seen. Thus, the growth is effectively blocked in the step growth regime (low supersaturations), whereas growth does occur but at a reduced rate, in the island nucleation regime.

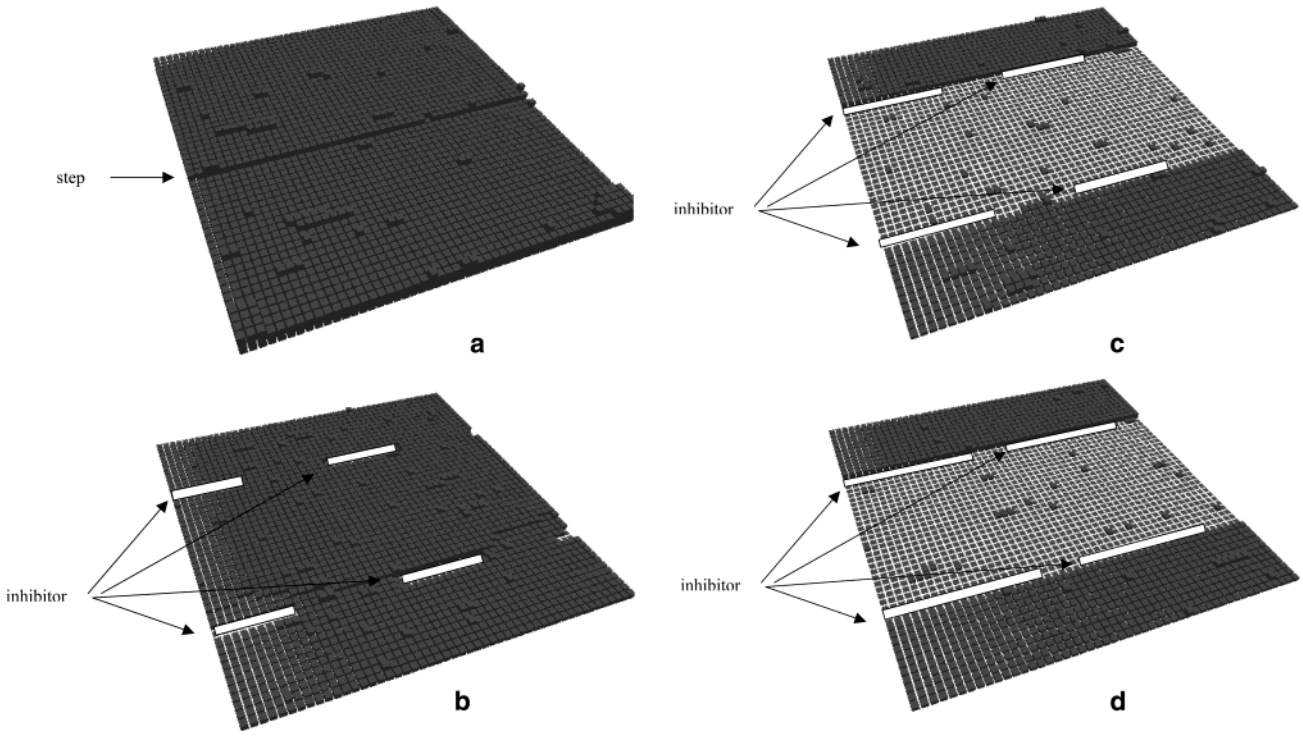

Figure 7. Configuration after 10^9 growth steps for (a) the clean surface and surfaces with four impurities of (b) length 10, (c) 15, and (d) 20 growth units. The bond strengths parallel (ϕ_y) and perpendicular (ϕ_x) to the molecule long axis are 0.7 and 10. 0 kT, respectively, and the excess chemical potential ($\Delta\mu$) is 0.2 kT. In the figures, each *n*-C_{28} molecule has been represented by a square grid point as this provides the clearest overview of the crystal growth; a more realistic depiction of the molecules would have long thin rectangles with the long axis (*y* direction) oriented perpendicular to the step

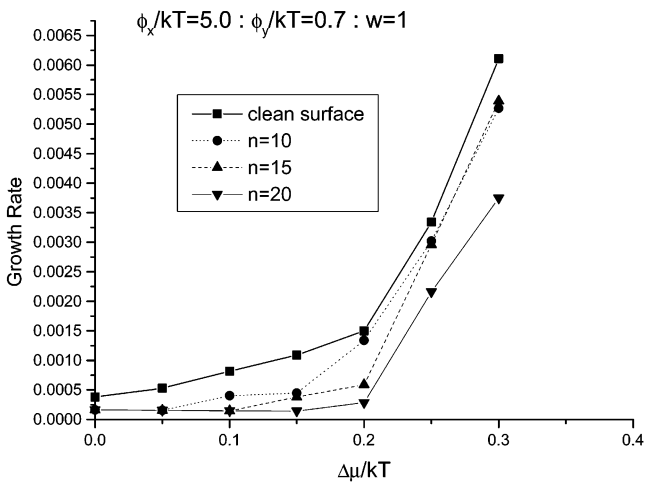

Figure 8. Growth rate versus excess chemical potential for MC simulations of growth with immobile impurities 1 growth unit wide ($w = 1$) and 10, 15, and 20 growth units long. The bond strengths parallel (ϕ_y) and perpendicular (ϕ_x) to the molecule long axis are 0.7 and 5.0 kT, respectively. The clean surface is included for comparison.

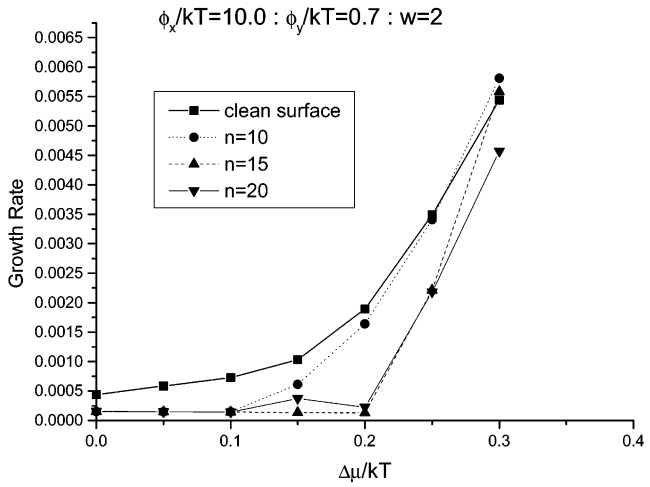

Figure 9. Growth rate versus excess chemical potential for MC simulations of growth with immobile impurities 2 growth units wide and 10, 15, and 20 growth units long. The bond strengths parallel (ϕ_y) and perpendicular (ϕ_x) to the molecule long axis are 0.7 and 10.0 kT, respectively. The clean surface is included for comparison.

Figures 8−10 show the equivalent growth plots using different values for ϕ_x and ϕ_y and different polymeric adsorption geometries. Reducing the footprint of the adsorbed polymer on the surface to $n \times 1$ lattice sites (Figure 8) has little effect on the inhibitor effectiveness. Likewise, doubling the side-by-side interaction energy (ϕ_x) has again little effect on either the growth rate or the inhibitor effectiveness (Figure 9). However, increasing the end-to-end interaction energy (ϕ_y) does have a significant effect on both the overall growth rate and the inhibitor effectiveness (Figure 10). In particular, it extends the step growth region and increases the supersaturation at which growth is blocked. Although this interaction energy is primarily a property of the *n*-C_{28} molecules, the interaction is mediated by the solvent. A solvent with a weaker interaction with the crystal than heptane would effectively increase ϕ_y and consequently increase the inhibitor effectiveness. For example, the vacuum MD simulations (Table 1) gave an estimate of $\phi_y = 8.3$ kJ mol^{-1} compared with the value of 1.75 kJ mol^{-1} found in liquid heptane. Thus, variations in the solvent composition could be used to increase the activity of the inhibitor. At the same time, however, this effect would also imply reduced solubility of the octacosane in the liquid and so would effectively increase the supersaturation. The balance of these two competing effects is not easy to predict.

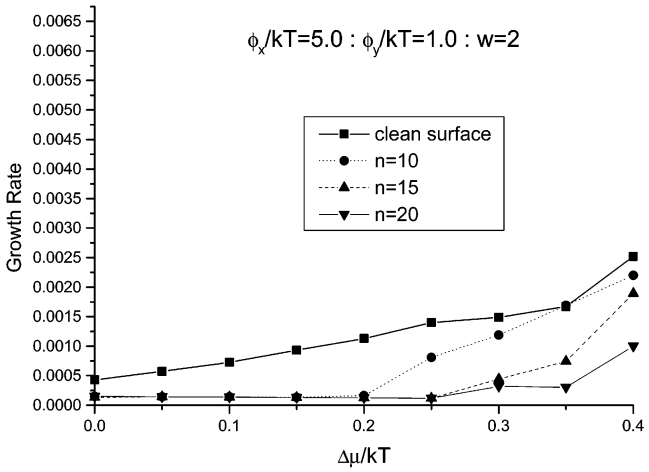

Figure 10. Growth rate versus excess chemical potential for MC simulations of growth with immobile impurities 2 growth units wide (ly) and 10, 15, and 20 growth units long (lx). The bond strengths parallel (ϕ_y) and perpendicular (ϕ_x) to the molecule long axis are 1.0 and 5.0 kT, respectively. The clean surface is included for comparison.

6. Conclusions

We have demonstrated that the most favorable position for nucleation of an alkane layer on an inhibited alkane surface is in a configuration that spans the inhibitor backbone, incommensurate with the underlying crystal. In addition, the mean energy of the molecules in a one-layer island on an inhibited surface was found to be significantly lower than the mean molecule energy of a one-layer island on a clean surface or indeed than molecules in the clean surface itself. Thus, the nucleation of a single layer on top of the inhibitor would occur relatively easily but further growth on this layer would create surface defects and would be slow.

Such incommensurate growth on adsorbed inhibitor molecules was shown to lead to a significant reduction in the interaction between the molecules adsorbed on top of the inhibitor and the surrounding crystal. Thus, the adsorption of polymers to the wax surface satisfies the conditions for growth blocking by immobile impurities: that is a strong interaction between the impurity and the substrate coupled with a weak interaction between the growth on the impurity and the surrounding crystal. To model this effect we have generalized a MC algorithm for crystal growth to allow for anisotropic molecular shape and then derived appropriate input parameters (specifically nearest-neighbor interaction energies) from molecular dynamics simulations. The MC simulations establish that the impurities do block crystal growth up to reasonable values of the supersaturation. In particular, they can completely inhibit step-growth and can slow the rate of growth in the island nucleation regime. The results are consistent with experiments, which found paraffin crystals grown in the presence of comb-shaped polymers were smaller and rougher than those grown from pure solution.[3]

A clear understanding of the inhibitor mechanism is essential for the efficient design of effective growth inhibitors. In this paper, we have established that the adsorption of inhibitor molecules on paraffin crystal surfaces leads to incommensurate growth and blocking of growth steps. For such a mechanism to be effective, it is necessary to design inhibitors that are readily adsorbed onto the crystal surface in a low energy conformation. It may also be possible to vary the inhibitor effectiveness by increasing the interaction energy between end-to-end neighbor alkane molecules ends by varying the solvent properties.

Acknowledgment. This work was supported by BP Exploration, U.K., under the Wax Attack program.

References and Notes

(1) Ding, X.; Qi, G.; Yang, S. *Polymer* **1999**, *40*, 4139.
(2) Hennessy, A. J.; Neville, A.; Roberts, K. J. *J. Cryst. Growth* **1999**.
(3) Kern, R.; Dassonville, R. *J. Cryst. Growth* **1992**, *116*, 191.
(4) Duffy, D. M.; Rodger, P. M. *Phys. Chem. Chem. Phys.* **2000**, *2*, 4804.
(5) Dorset, D. L. *J. Phys. Chem. B* **2000**, *104*, 8346−8350. Dorset, D. L.; *Energy Fuels* **2000**, *14*, 685−691.
(6) Duffy, D. M.; Rodger, P. M. *Phys. Chem. Chem. Phys.* **2002**, *4* 328.
(7) Cabrera, N.; Vermilyea, D. A. In *Growth and Perfection of Crystals*; Doremus, R., Roberts, B. W., Turnbull, D., Eds.; Wiley: New York, 1958; p 393.
(8) van Enckevort, W. J. P.; van der Berg, A. C. J. F.; Kreuwel, K. B. G.; Derksen, A. J.; Couto, M. S. *J. Cryst. Growth* **1996**, *166*, 156.
(9) van Enckevort, W. J. P.; van den Berg, A. C. J. F. *J. Cryst. Growth* **1998**, *183*, 441.
(10) Sangwal, K.; *J. Cryst. Growth* **1993**, *128*, 1236.
(11) Rashkovich, L.; N. V. Kronsky, *J. Cryst. Growth* **1997**, *182*, 434.
(12) Smith, W.; Forester, T. R. *J. Mol. Graph.* **1996**, *14*, 136.
(13) Allen, M. P.; Tildesley, D. J. *Computer Simulation of Liquids*; Clarendon Press: Oxford, 1987.
(14) Duffy, D. M.; Rodger, P. M. *Phys. Chem. Chem. Phys.* **2001**, *3*, 3580.
(15) Nyburg, S. C.; Gerson, A. R. *Acta Crystallogr. B* **1992**, *48*, 103. Shearer, H. M. M.; Vand, V. *Acta Crystallogr.* **1956**, *9*, 379.
(16) Moller, M. A.; Tildesley, D. J.; Kim, K. S.; Quirke, N. *J. Chem. Phys.* **1991**, *94*, 8390.
(17) Godwin, P. D.; Rodger, P. M. unpublished calculations.
(18) This is effectively an energy minimisation but with the advantage that *NVT* MD gives a finite lifetime for kinetic energy equilibration and so does allow some annealing over the small energy barriers associated with corrugations on the wax surface.
(19) Hartman, P.; Perdok, W. G. *Acta Crystallogr.* **1955**, *8*, 49; *Acta Crystallogr.* **1955**, *8*, 521; *Acta Crystallogr.* **1955**, *8*, 525.
(20) Gilmer, G. H.; Bennema, P. *J. Appl. Phys.* **1972**, *43*, 1347.